*Acta Chemica Scandinavica, 1993: 47: 979–984*
*Printed in Belgium – all rights reserved*


ACTA
CHEMICA SCANDINAVICA
*ISSN 0904-213X*

# NMR and Molecular Dynamics Study of the Tripeptide L-Pyroglutamyl-L-histidylglycine

Carl Henrik Görbitz*[,a] and Jostein Krane[b,c]

[a]Department of Chemistry, University of Oslo, P.O. Box 1033, Blindern, N-0315 Oslo 3, Norway, [b]Centre for Nuclear Magnetic Resonance, SINTEF, N-7034 Trondheim, Norway and [c]Department of Chemistry, University of Trondheim, AVH, N-7055 Dragvoll, Norway

Görbitz, C. H. and Krane, J., 1993. NMR and Molecular Dynamics Study of the Tripeptide L-Pyroglutamyl-L-histidylglycine. – Acta Chem. Scand. 47: 979–984.

The $^1$H spectrum of L-pyroglutamyl-L-histidylglycine in DMSO-$d_6$ and $^1$H and $^{13}$C NMR spectra in $D_2O$ at pH 4.26 to 8.90 have been analysed. $^3J_{HH}$ vicinal coupling constants were used to determine rotamer populations by means of the Karplus equation. Viable molecular geometries were obtained with the aid of molecular dynamics simulations including water as solvent. In DMSO and in aqueous solution at low pH two stable conformations were identified which both have an intramolecular hydrogen bond between the histidine side chain and the *C*-terminal carboxylate group.

A number of crystal structures of peptides with a pyroglutamyl group have been presented in the past.[1–11] This *N*-terminal residue is essential in the structure of thyrotropin-releasing hormone (TRH, pyroglutamyl-histidyl prolinamide) which has been the subject of extensive studies by NMR methods.[12–17] We present here an NMR-investigation of the biologically active analogue L-pyroglutamyl-L-histidylglycine (L-pGlu-L-His-Gly), Scheme 1.

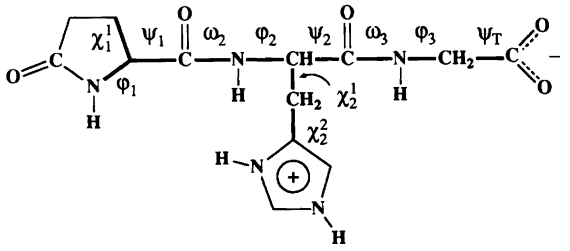

*Scheme 1.*

The molecular conformation can be described in terms of the eleven torsion angles indicated. These were divided into two groups and which are described separately. The first consists of $\varphi_1$, $\psi_1$, $\chi^1_1$, $\omega_2$ and $\varphi_2$ (pGlu part), the second of the six remaining angles (His-Gly part).

## Methods

*Chemicals.* L-pGlu-L-His-Gly acetate salt was purchased from Sigma and used as received.

*Preparation of solutions.* Three milligrams of the compound were dissolved in 0.6 ml of solvent for collection of $^1$H spectra while 20 mg were used for the $^{13}$C spectra. The approximate concentrations were 0.015 M and 0.10 M, respectively. For the pH-titration 25 mg of compound were dissolved in 90% $H_2O$–10% $D_2O$ with a phosphate buffer. The pH was adjusted by adding HCl or NaOH to the solution and measured with a radiometer pH/M62 pH-meter equipped with an Ingold combination electrode which was inserted into the NMR tube.

*NMR methods.* $^1$H (500 MHz) and $^{13}$C (100 MHz) spectra were collected on a Bruker AM 500 spectrometer equipped with an Aspect 3000 computer and were routinely measured using a $^1$H/$^{13}$C dual probe at a temperature of 21°C. The deuterium signal of the solvent provided the lock signal. The various two-dimensional experiments were performed using the standard Bruker pulse programmes. The water resonance signal was suppressed by the presaturation technique, while improved resolution was obtained by the double quantum technique.

*Calculations.* Spectral parameters were extracted from the second-order $^1$H spectra using the Bruker routine PANIC. Conformational searches were carried out with the SYBYL Version 5.41c program[18] on an Evans & Sutherland PS390 computer. Molecular dynamics simulations and other computational procedures were performed with the INSIGHTII Version 2.8 and DISCOVER Version 2.1.0 packages[19] on a Silicon Graphics Personal Iris workstation, employing the CVFF

* To whom correspondence should be addressed.

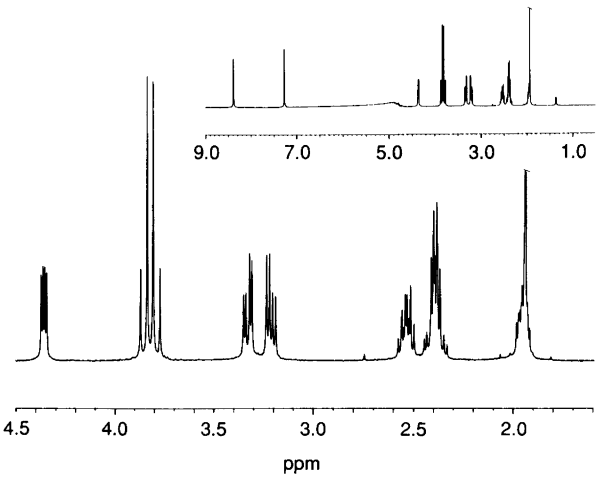


*Fig. 1.* Top: the 500 MHz $^1$H NMR spectrum of pGlu-His-Gly in $D_2O$. Bottom: detail of spectrum between 1.6 and 4.5 ppm. The acetate peak at 1.94 ppm has been reduced to less than 50% of original height in both spectra.

force field.[20,21] No Morse potentials or cross terms were used. The two model molecules pGlu-*N*-methyl-amide and His-Gly (with neutral *N*-terminal amino group and charged side chain and *C*-terminal carboxylate) were put inside $20^3$ Å$^3$ cubes and filled with 254 and 249 water molecules, respectively. After 30 steps of steepest descent energy minimization, molecular dynamics simulations at 300 K were carried out for 15 ps, of which the first 5 ps served as equilibration periods. The time step was 1 fs,

*Table 1.* $^1$H and $^{13}$C chemical shifts (ppm) of L-pGlu-L-His-Gly in $D_2O$ and DMSO.

| Atom | $D_2O$ | DMSO |
|---|---|---|
| pGlu α-H | 4.39 | 4.03 |
| pGlu β-$H_A$ | 1.98 | —[a] |
| pGlu β-$H_B$ | 2.57 | — |
| pGlu γ-$H_A$ | 2.41 | — |
| pGlu γ-$H_B$ | 2.44 | — |
| pGlu N-H | 7.89[b] | 7.82 |
| His α-H | ~4.85[c] | 4.46 |
| His β-$H_A$ | 3.25 | 2.88 |
| His β-$H_B$ | 3.36 | 2.97 |
| His 5-H | 7.30 | 6.80 |
| His 2-H | 8.41 | 7.62 |
| His N-H | 8.51[b] | 8.11 |
| Gly α-$H_A$ | 3.83 | 3.60 |
| Gly α-$H_B$ | 3.88 | 3.75 |
| Gly N-H | 8.36[b] | 8.26 |
| pGlu $C^\alpha$ | 59.62 | |
| pGlu $C^\beta$ | 27.91 | |
| pGlu $C^\gamma$ | 31.86 | |
| His $C^\alpha$ | 55.36 | |
| His $C^\beta$ | 30.01 | |
| His C-4 | 132.24 | |
| His C-5 | 120.40 | |
| His C-2 | 137.23 | |
| Gly $C^\alpha$ | 46.08 | |

[a] Not calculated. [b] Measured at pH = 4.26. [c] Estimated value from heteronuclear correlation spectrum.

*Table 2.* $^1$H NMR coupling constants (Hz) in L-pGlu-L-His-Gly.

| Coupling | $D_2O$ | DMSO |
|---|---|---|
| $^3J_{\text{pGlu α-H, pGlu β-H}_A}$ | 4.75 | 4.05 |
| $^3J_{\text{pGlu α-H, pGlu β-H}_B}$ | 9.27 | 8.63 |
| $^3J_{\text{pGlu β-H}_A\text{, pGlu β-H}_B}$ | −13.41 | —[a] |
| $^3J_{\text{pGlu β-H}_A\text{, pGlu γ-H}_A}$ | 10.02 | — |
| $^3J_{\text{pGlu β-H}_A\text{, pGlu γ-H}_B}$ | 7.23 | — |
| $^3J_{\text{pGlu β-H}_B\text{, pGlu γ-H}_A}$ | 5.60 | — |
| $^3J_{\text{pGlu β-H}_B\text{, pGlu γ-H}_B}$ | 10.16 | — |
| $^3J_{\text{pGlu γ-H}_A\text{, pGlu γ-H}_B}$ | −17.48 | — |
| $^3J_{\text{pGlu α-H, pGlu NH}}$ | —[b] | ~0.8 |
| $^3J_{\text{His α-H, His β-H}_A}$ | 7.81 | 7.88 |
| $^3J_{\text{His α-H, His β-H}_B}$ | 5.89 | 4.91 |
| $^3J_{\text{His β-H}_A\text{, His β-H}_B}$ | −15.29 | −14.66 |
| $^3J_{\text{His α-H, His NH}}$ | 7.4[c,d] | 7.94 |
| $^3J_{\text{Gly α-H}_A\text{, Gly α-H}_B}$ | −17.24 | −17.25 |
| $^3J_{\text{Gly α-H}_A\text{, Gly NH}}$ | 5.81[c] | 5.49 |
| $^3J_{\text{Gly α-H}_B\text{, Gly NH}}$ | 5.92[c] | 5.79 |

[a] Not calculated. [b] Not resolved. [c] Measured at pH = 4.26. [d] From splitting of N-H peak.

and periodic boundary conditions were used with 10.0 Å as the cut-off distance. All simulations were run at 300 K.

## Results

The peaks in the $D_2O$ $^1$H spectrum (Fig. 1) were assigned combining knowledge of the typical patterns of the individual amino acids with $^1$H homonuclear *J*-correlated spectroscopy (COSY). The resonance for His-$H^\alpha$ is under the suppressed water peak at ~5 ppm in Fig. 1, but appeared in the heteronuclear chemical-shift correlated spectrum which also established the assignment of the $^{13}$C spectrum. The spectrum in DMSO is similar to the one in water, and the COSY-spectrum has the same characteristics. The titration of the molecule in $D_2O$–$H_2O$ allowed determinations of pH-dependent $^3J_{NH^\alpha-CH^\alpha}$ coupling constants in aqueous solution. Chemical shifts and coupling constants for the molecule in water and DMSO are listed in Tables 1 and 2, respectively.

## Discussion

*pGlu conformation.* Of the five torsion angles shown in Scheme 1, $\chi_1^1$ and $\varphi_1$ are determined by pGlu ring puckering, $\omega_2$ is *trans* and close to 180°, while $\psi_1$ and $\varphi_2$ describe the chain orientation. The pGlu five-membered ring can adopt two stable non-planar conformations with the $H^\alpha$-atom in either a pseudoaxial (I) or a pseudoequatorial (II) position (Scheme 2), which are equally abundant in crystal structures (Table 3).

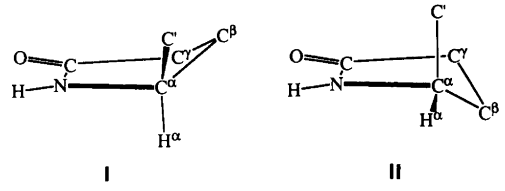


*Scheme 2.*

*Table 3.* Ring puckering and torsion angles in crystal structures of pGlu-residues.

| Compound | Puckering[a] | $\varphi_1$ | $\psi_1$ | $\varphi_2$ | $\psi_2$ | $\chi^1_2$ | $\chi^2_2$ | Ref. |
|---|---|---|---|---|---|---|---|---|
| L-pGlu | I | 138.2 | | | | | | 1 |
| | I | 128.5 | | | | | | 1 |
| | I | 138.6 | | | | | | 1 |
| | I | 142.7 | | | | | | 2 |
| | pl | 125.3 | | | | | | 2 |
| | I | 142.7 | | | | | | 3 |
| L-pGlu-*N*, *N'*-dicyclohexylurea | II | 90.5 | | | | | | 4 |
| L-pGlu-$NHCH_3$ | I | 134.1 | 168 | | | | | 5 |
| L-pGlu-β-(2-thienyl)-L-Ala-L-Pro-$NH_2$ | II | 98.5 | 18 | −96 | 133 | −66 | 71 | 6 |
| | II | 106.4 | 12 | −97 | 122 | −66 | 72 | 6 |
| | II | 104.7 | 8 | −92 | 121 | −63 | 70 | 7 |
| | II | 107.2 | 10 | −97 | 124 | −67 | 71 | 7 |
| L-pGlu-L-His methyl ester | I | 131.9 | 155 | −81 | 139 | −178 | 57 | 8 |
| L-pGlu-L-His-L-Pro-$NH_2$ tartrate · $H_2O$ | II | 108.0 | 146 | −70 | 137 | −163 | 62 | 9 |
| L-pGlu-L-Phe-L-Pro-$NH_2$ | II | —[b] | 144 | ≈ −90[b] | 132 | 180 | −71 | 10 |
| L-pGlu-L-Ala | I/pl | 123.9 | 166 | −90 | | | | 11 |

[a] See Scheme 1, pl = planar. [b] Not published, the value for $\varphi_2$ is a rough estimate from the figure in the original paper.[19]

Associated values for the $\chi^1_1$ and $\varphi_1$ torsion angles are ≈ −25°/105° and 25°/137°, respectively. The molecular dynamics diagram for $\chi^1_1$ in the model peptide pyroglutamyl-*N*-methylamide in Fig. 2 shows numerous transitions between the two envelope forms during the 10 ps simulation. This means that the flip-flop rate is fast on the NMR timescale, explaining the sharp peaks in the $^1$H NMR spectra. Fig. 3 shows the molecular dynamics diagram for $\psi_1$. Prior to solvation, the molecule was minimized *in vacuo* to give $\psi_1 = -156.6°$ (203.6°), but in the solvated system $\psi_1$ is around 80–160° with 44° and 196° as extreme limits. The results compare nicely to observed values in crystal structures, Table 3, which also include structures with $\psi_1$ close to 0°.

The 7.4 Hz $^3J_{NH-C^\alpha H}$ coupling constant observed for the His residue in aqueous solution (Table 2) was used to determine the possible values for $\varphi_2$. According to empirical curves there are two possible geometries with $\varphi_2$ close to −155° or −85°.[22] Roughly the same coupling was observed for the His residue in TRH for which it has been suggested that the extended structure is most favoured.[12,15,16] We believe that although both conformations can exist in solution, the conformation with $\varphi_2 = -85°$ may be the most important. This assumption is based on two observations. (1) With $\varphi_2 \approx -85°$, rotation around the $C^\alpha$–$C^\beta$ bond ($\chi^1_1$) is sterically unhindered. This is unlike the situation for $\varphi_2 \approx -155°$, as the side chain rotamer with $\chi^1_2 = -60°$ cannot easily be obtained owing to steric conflict with the main chain and with the pGlu ring (particularly for conformations with $\psi_1$ near 0°). Thus, the bent conformation with $\varphi_2 \approx -85°$ may be entropically favoured in solution. (2) In crystal structures of pGlu-Xaa peptides, $\varphi_2$ is always close to −85° (Table 3). Furthermore, in linear Xaa-His peptides $\varphi_2$ is most commonly observed around this value.[8,9,23,24] Thus, the crystallographic material indicates that for pGlu-His,

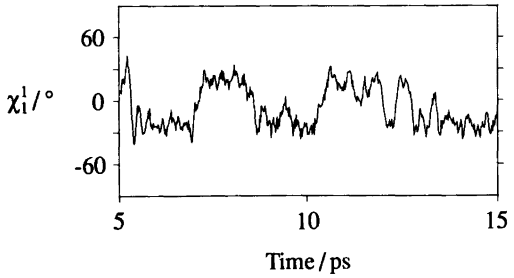


*Fig. 2.* Time profile for the N–$C^\alpha$–$C^\beta$–$C^\gamma$ ($\chi^1$) torsion angle in the five-ring of pGlu-*N*-methylamide showing transitions between the puckered forms I ($\chi^1 \approx -25°$) and II ($\chi^1 \approx 25°$).

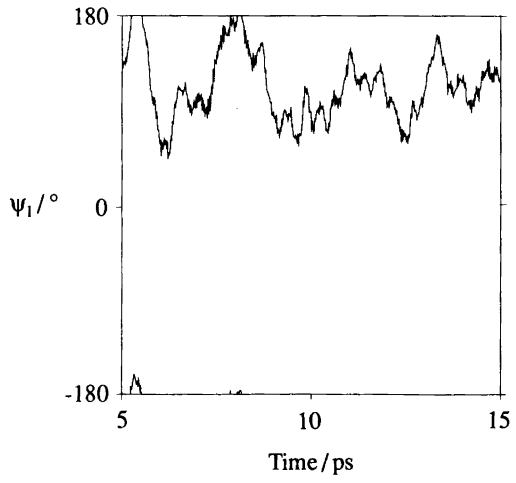


*Fig. 3.* Time profile for the $\psi_1$ torsion angle in pGlu-*N*-methylamide.

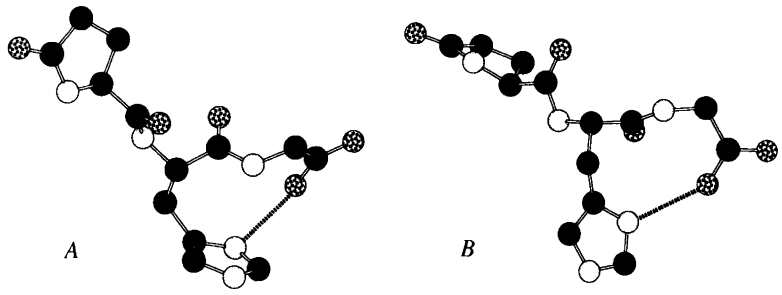


*Fig. 4.* pGlu-His-Gly in the two hydrogen-bonded conformations **A** and **B** described in the text. H-atoms have been omitted for clarity. Both molecules are shown with puckering I for the pGlu ring.

$\varphi_2$ around $-85°$ is most favourable, at least in the solid phase.

In the pGlu part of the molecule neither chemical shifts nor coupling constants change appreciably in the pH interval 4.26–8.90, indicating that no major conformational changes take place during titration.

*His-Gly conformation.* The charged imidazole group of the His side chain ($HisH^+$) is an excellent hydrogen bond donor, while the *C*-terminal carboxylate group of the adjacent Gly residue is an equally potent hydrogen-bond acceptor. These two groups can interact to form an intramolecular hydrogen bond. Such a contact is only possible for certain conformations of the molecule, or rather a subspace of the conformational space formed by the six torsion angles $\chi_2^1$, $\chi_2^2$, $\psi_2$, $\omega_3$, $\varphi_3$ and $\psi_T$ (Scheme 1). Relevant parameter-sets were sampled using the SYSTEMATIC SEARCH facility of the SYBYL program, in which each torsion angle is incremented in steps within a selected range. In the present search, an increment of 10° was used for each angle, except for $\omega_3$ with a 5° step within the interval [175°, 185°] (*trans* peptide bond only, as expected the presence of a *cis* form was not indicated by the NMR data). Other ranges were $[50°, 70°] + [170°, 190°] + [-70°, -50°]$ for $\chi_2^1$, $[70°, 110°] + [-110°, -70°]$ for $\chi_2^2$, and [0°, 350°] for $\psi_2$, $\varphi_3$ and $\psi_T$, giving a theoretical total of $1.3 \times 10^7$ combinations. Geometries at the $C^\alpha$-atoms and for the peptide bond were taken from Ref. 25. Data for carboxylate group dimensions were taken from a survey of carboxylate crystal structures.[26] Only $N^\pi$-H is a potential hydrogen-bond donor in the interaction, and the objective of the search was maintained by constraining the $N^\pi \cdots O'$ distance to the interval [2.56 Å, 2.73 Å], derived from a 2.664 Å average distance reported for a survey of crystal structures.[27]

The search identified essentially two different conformations **A** and **B** for the $HisH^+$-Gly moiety, Fig. 4. They were represented by 2360 and 1187 torsion angle combinations respectively, illustrating considerable flexibility for the 10-membered rings formed by the intramolecular hydrogen bonds. The torsion angles were confined to the following intervals: (**A**) $\psi_2$: [130°, 150°], $\varphi_3$: $[-100°, -50°]$, $\psi_T$: $[-40°, 30°]$, $\chi_2^1$: [180°, 190°], $\chi_2^2$: $[-90°, -70°]$ (**B**) $\psi_2$: [150°, 170°], $\varphi_3$: $[-100°, -50°]$, $\psi_T$: $[-50°, 50°]$, $\chi_2^1$: [60°, 70°], $\chi_2^2$: [70°, 90°]. The most notable differences occur for the His side chain orientation which is *trans* for **A** and *gauche*$^+$ for **B** and opposite signs for $\chi_2^2$. Among $-HisH^+$-Xaa– crystal structures TRH[9] (pGlu-His-Gly) displays an **A**-type

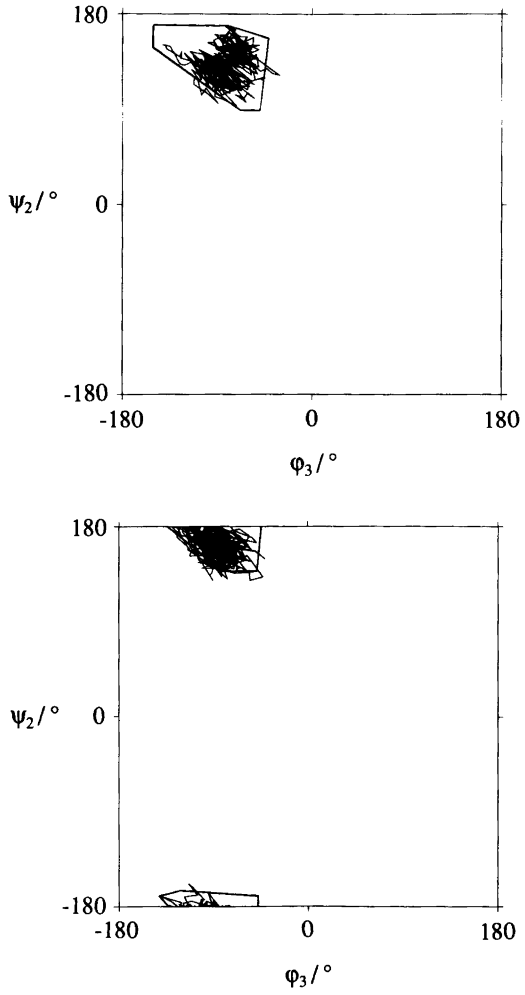


*Fig. 5.* $\psi_2/\varphi_3$ trajectories for conformations **A** (top) and **B** (bottom) during the molecular dynamics simulations. The solid lines limit the regions observed for **A** and **B** in the systematic search for H-bonded conformations with the SYBYL program. Note that this is not a regular Ramachandran plot since ψ and φ-values for two different residues are displayed.

*Table 4.* $^3J_{\alpha\text{-},\beta\text{-H}}$ coupling constants (Hz) and rotamer populations for the $C^\alpha$–$C^\beta$ bond of the L-His residue.

| | | | Rotamer populations[a] | | | | | |
|---|---|---|---|---|---|---|---|---|
| | | | Alternative 1 | | | Alternative 2 | | |
| pH | $^3J_{\alpha\text{-H},\beta\text{-H}}$ | | *trans* | *gauche*$^-$ | *gauche*$^+$ | *trans* | *gauche*$^-$ | *gauche*$^+$ |
| 4.26 | 5.99 | 7.48 | 0.48 | 0.29 | 0.24 | 0.34 | 0.47 | 0.18 |
| 5.72 | 5.95 | 7.57 | 0.49 | 0.28 | 0.23 | 0.34 | 0.48 | 0.18 |
| 6.25 | 5.86 | 7.81 | 0.52 | 0.27 | 0.22 | 0.34 | 0.51 | 0.15 |
| 6.68 | 5.70 | 8.21 | 0.56 | 0.24 | 0.20 | 0.33 | 0.56 | 0.11 |
| 7.11 | 5.52 | 8.68 | 0.62 | 0.21 | 0.17 | 0.33 | 0.61 | 0.06 |
| 7.70 | 5.37 | 9.10 | 0.67 | 0.19 | 0.14 | 0.33 | 0.66 | 0.01 |
| 8.11 | 5.33 | 9.25 | 0.69 | 0.18 | 0.13 | 0.33 | 0.68 | 0.00 |
| 8.90 | 5.32 | 9.33 | 0.70 | 0.18 | 0.12 | 0.33 | 0.69 | −0.02 |
| DMSO | 4.91 | 7.88 | 0.48 | 0.16 | 0.35 | 0.21 | 0.54 | 0.25 |

[a] Calculations were based on the equations reported by Feeney:[29]
$J_{AX} = 4.1pI + 11.7pII + 2.9pIII$
$J_{BX} = 12.0pI + 2.1pII + 4.7pIII$
$pI + pII + pIII = 1.0$
where $pI = trans$, $pII = gauche^+$ and $pIII = gauche^-$.

conformation, L-Met-L-Glu-L-His-L-Phe[24] is found in a **B**-type orientation, while there is no intramolecular H-bond in the L-Asp-L-Phe L-His-Gly cocrystal.[28]

**A**- and **B**-type H-bonds were then built into the model peptide $HisH^+$-Gly and submitted to molecular dynamics simulations. The two resulting $\psi_2/\varphi_3$-trajectories are shown in Fig. 5. It can be seen that only one $\psi_2/\varphi_3$-region is observed for each conformation, and that the agreement with the regions previously obtained with stiff rotor models in the SYBYL search is excellent. It should be noted that when $HisH^+$-Gly zwitterion peptides were minimized *in vacuo*, the overall energy of the molecule is totally dominated by the contribution from the electrostatic term in the force-field equation. The resulting molecular geometries deviate substantially from those obtained in the molecular dynamics runs, with grossly non-planar imidazole rings and peptide bonds (**A**: $\psi_2 = 111.1°$, $\omega_2 = 144.8$, $\varphi_3 = -81.7°$, **B**: $\psi_2 = 160.1$, $\omega_2 = 145.4$, $\varphi_3 = -80.2$). These results for $\psi_2/\varphi_3$ and previous results for $\psi_1$ clearly demonstrate that the inclusion of solvent interactions is essential for force-field studies of polar molecular systems in solution.

Having established the viability of $HisH^+ \cdots {}^-OOC$ intramolecular interactions, we were interested to see whether they were indicated by the NMR data. The first step in this procedure was to study the His side-chain rotamer populations by the Karplus equation.[29] The coupling constants $H\text{–}C^\alpha C^\beta\text{–}H_A$ and $H\text{–}C^\alpha C^\beta\text{–}H_B$ were known, and rotamer populations around the $C^\alpha$–$C^\beta$ bond could be calculated by considering only the three staggered positions. As no stereochemical assignment of the two β-protons had been made, two sets of distributions are possible, Table 4. There is good evidence that the left column shows the correct distributions, given the unnatural negative population for *gauche*$^+$ at pH 8.90. The high fractions of *gauche*$^+$ and *trans* in DMSO is compatible with dominance of conformations **A** and **B** defined above. At low pH a similar distribution is observed in water, but as the pH is raised and $N^\pi$ is deprotonated, the number of hydrogen-bonded structures dwindles and the *gauche*$^+$ rotamer loses some of its importance. Without any obvious reason, the same pattern occurs for *gauche*$^-$, leaving *trans* as the dominant species at high pH.

We considered next the chemical shift difference, Δδ, between the two glycyl protons. It has been proposed that the magnitude of Δδ is indicative of the degree of conformational homogeneity.[30] In DMSO Δδ is as large as 0.15 ppm, thus suggesting that the bulk of the molecules are confined to a small number of conformations, most likely those stabilized by hydrogen bonding. In water Δδ

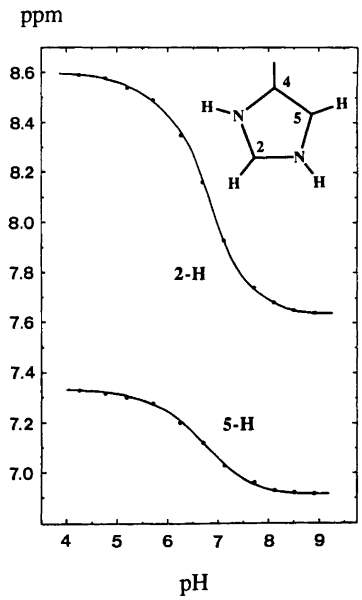


*Fig. 6.* $^1H$ NMR titration curves for the imidazole 5-H and 2-H ring protons of pGlu-His-Gly in 90% $H_2O$–10% $D_2O$.

is 0.080 ppm at pH 4.26, but drops even further to 0.047 at pH 8.90.

Evidence for intramolecular hydrogen bonding also comes from the $pK_a$-value of the imidazole group. All resonances for atoms in the His-residue move during titration, protons to higher field, carbon atoms in the opposite direction. Titration curves for ring protons shown in Fig. 6 appear as expected, with titration shifts 0.95 ppm for C2-H and 0.42 ppm for C5-H. The derived $pK_a$-value is 6.85, significantly higher than observed for free His ($\sim$6.16).[31] This increase can be attributed to the participation of the N$\pi$-H proton in a strong, presumably intramolecular hydrogen bond. The $pK_a$-value and the titration curves are almost identical with those reported for the tripeptide Gly-L-His-Gly ($pK_a = 6.90$)[32] where similar interactions may prevail.

## Concluding remarks

The NMR and molecular dynamics data for L-pGlu-L-His-Gly in DMSO and in water at low pH are consistent with the predominance of two different conformations which both incorporate intramolecular $HisH^+ \cdots$ carboxylate hydrogen-bonds into 10-membered ring systems, Fig. 4. The orientation of the main chain at high pH may be relatively extended, with a predominant *trans* orientation for the His side chain. The geometry of the *N*-terminal part of the molecule is independent of solvent and pH with $\psi_1$ in the range 80–160°, $\varphi_2$ presumably around $-85°$, and with rapid flip-flopping between the two puckered forms for the pGlu ring.

## References


1. van Zoeren, E., Oonk, H. A. J. and Kroon, J. *Acta Crystallogr., Sect. B 34* (1978) 1898.
2. Taira, Z. and Watson, W. H. *Acta Crystallogr., Sect. B 33* (1977) 3823.
3. Patthabi, V. and Venkatesan, K. *J. Chem. Soc., Perkin Trans. 2* (1974) 1085.
4. Bechtel, F., Bideau, J. P. and Cotrait, M. *Cryst. Struct. Commun. 8* (1979) 815.
5. Aubry, A., Marraud, M., Protas, J. and Néel, J. *C.R. Acad. Sci. Paris, 274 C* (1972) 1378.
6. Norrestam, R., Stensland, B. and Castensson, S. *Acta Chem. Scand., Ser. A 38* (1984) 473.
7. Stensland, B. and Castensson, S. *J. Mol. Biol. 161* (1982) 257.
8. Cotrait, M. and Allard, M. *C. R. Acad. Sci. Paris, 276 C* (1973) 1671.
9. Kamiya, K., Takamoto, M., Wada, Y., Fujino, M. and Nishikawa, M. *J. Chem. Soc., Chem. Commun.* (1980) 438.
10. Stezowski, J. J., Bürvenich, C. and Voelter, W. *Angew. Chem. 91* (1979) 243.
11. Ramasubbu, N. and Parthasarathy, R. *Int. J. Peptide Protein Res. 33* (1989) 328.
12. Fermandjian, S., Pradelles, P., Fromageot, P. and Dunand, J.-J. *FEBS Lett. 28* (1972) 156.
13. Deslauries, R., Walter, R. and Smith, I. C. P. *Biochem. Biophys. Res. Commun. 53* (1973) 244.
14. Feeney, J., Bedford, G. R. and Wessels, P. L. *FEBS Lett. 42* (1974) 347.
15. Donzel, B., Rivier, J. and Goodman, M. *Biopolymers 13* (1974) 2631.
16. Montagut, M., Lemanceau, B., Bellocq, A.-M. *Biopolymers 13* (1974) 2615.
17. Haar, W., Fermandjian, S., Vicar, J., Blaha, K. and Fromageot, P. *Proc. Natl. Acad Sci. USA 72* (1975) 4948.
18. Tripos Associates Inc., 1699 South Hanley Rd, St. Lois, Missouri 63144.
19. Biosym Technologies Inc., 10065 Barnes Canyon Rd, San Diego, CA 92121.
20. Hagler, A. T. and Lifson, S. *J. Am. Chem. Soc. 96* (1974) 5319.
21. Dauber-Osguthorpe, P., Roberts, V. A., Osguthorpe, D. J., Wolf, J., Genest, M. and Hagler, A. T. *Proteins 4* (1988) 31.
22. Pardi, A., Billeter, M. and Wüthrich, K. *J. Mol. Biol. 180* (1984) 741.
23. Aubry, A., Vlassi, M. and Marraud, M. *Int. J. Peptide Protein Res. 28* (1986) 637.
24. Admiraal, G. and Vos, A. *Acta Crystallogr., Sect. C 39* (1983) 82.
25. Ashida, T., Tsunogae, Y., Tanaka, I. and Yamane, T. *Acta Crystallogr., Sect. B 43* (1987) 212.
26. Görbitz, C. H. *Unpublished data.*
27. Görbitz, C. H. *Acta Crystallogr., Sect. B 45* (1989) 390.
28. Görbitz, C. H. and Etter, M. C. *Acta Crystallogr., Sect. C 49* (1993). *In press.*
29. Feeney, J. *J. Magn. Reson. 21* (1976) 473.
30. Beeson, C. and Dix, T. A. *J. Chem. Soc., Perkin Trans. 2* (1991) 1913.
31. Sachs, D. H., Schechter, A. N. and Cohen, J. S. *J. Biol. Chem. 246* (1971) 6576.
32. Markley, J. L. *Acc. Chem. Res. 8* (1975) 70.


Received December 14, 1992.